

$\Lambda^*(1405)$ -matter: stable or unstable?

J. Hrtánková^{a,b}, N. Barnea^c, E. Friedman^c, A. Gal^{c,*}, J. Mareš^a,
M. Schäfer^{a,b}

^a*Nuclear Physics Institute, 25068 Řež, Czech Republic*

^b*Faculty of Nuclear Sciences and Physical Engineering,*

Czech Technical University in Prague, 115 19 Prague 1, Czech Republic

^c*Racah Institute of Physics, The Hebrew University, 91904 Jerusalem, Israel*

Abstract

A recent suggestion [PLB 774 (2017) 522] that purely- $\Lambda^*(1405)$ nuclei provide the absolute minimum energy in charge-neutral baryon matter for baryon-number $A \gtrsim 8$, is tested within RMF calculations. A broad range of Λ^* interaction strengths, commensurate with $(\bar{K}\bar{K}NN)_{I=0}$ binding energy assumed to be of order 100 MeV, is scanned. It is found that the binding energy per Λ^* , B/A , saturates for $A \gtrsim 120$ with values of B/A considerably below 100 MeV, implying that $\Lambda^*(1405)$ matter is highly unstable against strong decay to Λ and Σ hyperon aggregates. The central density of Λ^* matter is found to saturate as well, at roughly twice nuclear matter density. Moreover, it is shown that the underlying very strong $\bar{K}N$ potentials, fitted for isospin $I = 0$ to the mass and width values of $\Lambda^*(1405)$, fail to reproduce values of single-nucleon absorption fractions deduced across the periodic table from K^- capture-at-rest bubble chamber experiments.

Keywords: strange matter, $\Lambda^*(1405)$ resonance, kaonic atoms, RMF

1. Introduction

Strangeness (\mathcal{S}) provides for extension of standard nuclear matter to strange matter in which SU(3)-octet hyperons (Λ, Σ, Ξ) may prove as abundant as nucleons [1]. Particularly interesting at present is the role of hyperons in the composition of the neutron star interior, the so called ‘hyperon puzzle’ [2]. Little is known about the possible role of higher-mass hyperons in

*corresponding author: Avraham Gal, avragal@savion.huji.ac.il

hadronic matter. However, it was recently suggested by Akaishi and Yamazaki (AY) [3] that purely- $\Lambda^*(1405)$ aggregates become increasingly bound with the number $A = -\mathcal{S}$ of Λ^* constituents, reaching absolute stability for $A \gtrsim 8$. This suggestion for which we found no documented supporting calculations beyond $A = 2$ follows a similar conjecture made already in 2004 [4]. It is worth recalling that solving the A -body Schrödinger equation for purely attractive $\Lambda^*\Lambda^*$ interactions will necessarily lead to collapse, with the binding energy per Λ^* , B/A , and the central Λ^* density $\rho(r \approx 0)$ diverging as A increases. This immediately raises the question whether AY perhaps just overlooked this basic many-body aspect of the Schrödinger equation in asserting that purely- Λ^* matter becomes absolutely stable for some given value of A . Therefore the issue of stability has to be checked within calculational schemes that avoid many-body collapse. A commonly used approach in nuclear and hadronic physics that avoids collapse and provides sufficiently faithful reproduction of nuclear binding energies and densities is the Relativistic Mean Field (RMF) approach [5] which is used here.

In this Letter, we show within RMF calculations in which strongly attractive $\Lambda^*\Lambda^*$ interactions are generated through scalar meson (σ) and vector meson (ω) exchanges that both B/A , the Λ^* -matter binding energy per baryon, and the central density $\rho(r \approx 0)$ saturate for values of A of order $A \sim 100$. For the case considered here, B/A saturates at values between roughly 30 to 80 MeV, depending on details of the RMF modeling, and the associated central densities saturate at values about twice nuclear-matter density. This leaves Λ^* aggregates highly unstable against strong interaction decay governed by two-body conversion reactions such as $\Lambda^*\Lambda^* \rightarrow \Lambda\Lambda, \Sigma\Sigma$.

The plan of this note is as follows. In Sect. 2 we briefly review several few-body calculations of \bar{K} nuclear quasibound states, including those based on energy independent strongly attractive $\bar{K}N$ potentials as advocated by AY, in order to introduce plausible input values for the $\Lambda^*\Lambda^*$ binding energy ($B_{\Lambda^*\Lambda^*}$) used to determine the strength of the scalar and vector meson-exchange couplings applied in our subsequent RMF calculations. In Sect. 3 we question the validity of such energy independent strongly attractive $\bar{K}N$ interactions by checking their ability to reproduce the single-nucleon absorption fractions deduced from K^- capture observations in bubble chamber experiments. RMF calculations of purely- Λ^* nuclei are reported in Sect. 4, showing clearly how B/A and ρ saturate as a function of A , thereby leaving Λ^* matter highly unstable. A brief Conclusion section summarizes our results with some added discussion.

2. \bar{K} nuclear quasibound states

Table 1: $(\bar{K}N)_{I=0}$, $(\bar{K}NN)_{I=1/2}$ and $(\bar{K}\bar{K}NN)_{I=0}$ binding energies B (in MeV) calculated using energy dependent (E-dep.) [9] and energy independent (E-indep.) [10] $\bar{K}N$ potentials. $(\bar{K}\bar{K}NN)_{I=0}$ binding energies are transformed in the last row to $B_{\Lambda^*\Lambda^*}$ values.

\bar{K} nuclei	(E-dep.)	(E-indep.) _a	(E-indep.) _b
$(\bar{K}N)_{I=0}$	11.4	26.6	64.2
$(\bar{K}NN)_{I=1/2}$	15.7	51.5	102
$(\bar{K}\bar{K}NN)_{I=0}$	32.1	93	190
$\Lambda^*\Lambda^*$	9.3	40	62

The $I = 0$ antikaon-nucleon ($\bar{K}N$) interaction near threshold is attractive and sufficiently strong to form a quasibound state. Using a single-channel energy independent $\bar{K}N$ potential this quasibound state has been identified by AY, e.g. in Refs. [6, 7], with the $J^P = (1/2)^- \Lambda^*(1405)$ resonance about 27 MeV below the K^-p threshold. In contrast, in effective field theory (EFT) approaches where the $\bar{K}N$ effective single-channel potential comes out energy dependent, reflecting the coupling to the lower-energy $\pi\Sigma$ channel, this $\bar{K}N$ quasibound state is bound only by about 10 MeV [8]. The difference between $\bar{K}N$ binding energies gets compounded in multi- $\bar{K}N$ quasibound states predicted in these two approaches, as demonstrated for $(\bar{K}\bar{K}NN)_{I=0}$ in Table 1 by comparing binding energies B listed in the (E-dep.) column with those listed in the (E-indep.) columns. Regarding these two columns, we note that the binding energies listed in column (E-indep.)_b arise by fitting the $(\bar{K}N)_{I=0}$ potential strength such that it reproduces the value $B(\bar{K}NN)_{I=1/2} = 102$ MeV derived from the DISTO experiment [11]. This derivation was challenged subsequently by the HADES Collaboration [12]. The most recent J-PARC E15 [13] dedicated experiment derives a value of $B(\bar{K}NN)_{I=1/2} = 47 \pm 3_{-6}^{+3}$ MeV. Therefore, when studying energy independent $\bar{K}N$ potentials, we will keep to the (E-indep.)_a scenario that also identifies the $(\bar{K}N)_{I=0}$ quasibound state with the $\Lambda^*(1405)$ resonance observed 27 MeV below threshold. This identification plays an essential role in the earlier Akaishi and Yamazaki works, Refs. [6, 7]. It is worth noting that the more refined state-of-the-art chiral EFT approaches, with low-energy constants fitted to *all* existing K^-p low-energy data, produce two $(\bar{K}N)_{I=0}$

quasibound states [14], the narrower and least bound of which is consistent with the (E-dep.) column of Table 1.

3. Kaonic atoms test

Here we confront the (E-indep.)_a scenario of the last section with the broad data base of kaonic atoms which are known to provide a sensitive test of $\bar{K}N$ interaction models near threshold [15]. In the last decade several chiral EFT models of the $\bar{K}N$ interaction provided K^-N scattering amplitudes based on fits to low energy K^-p data, including kaonic hydrogen from the SIDDHARTA experiment [16, 17]. Kaonic atom potentials based on such single-nucleon amplitudes within a sub-threshold kinematics approach are generally unable to fit the kaonic atom data unless an additional phenomenological density dependent amplitude representing multi-nucleon processes is introduced. In a recent work [18] this procedure was applied to several chiral EFT $\bar{K}N$ model amplitudes. Good fits to the data were reached with χ^2 values of 110 to 120 for 65 data points. Considering that the data come from four different laboratories, covering the whole of the periodic table, these χ^2 values are quite satisfactory. This procedure was extended to include also $\bar{K}N$ amplitudes generated from the energy independent $\bar{K}N$ potentials used by Yamazaki and Akaishi (YA) [7] (in MeV),

$$\begin{aligned} V_{\bar{K}N}^{I=0}(r) &= (-595 - i83) \exp[-(r/0.66 \text{ fm})^2], \\ V_{\bar{K}N}^{I=1}(r) &= (-175 - i105) \exp[-(r/0.66 \text{ fm})^2]. \end{aligned} \tag{1}$$

These potentials approximate reasonably the (E-indep.)_a scenario of the last section. The corresponding $\bar{K}N$ amplitudes are shown in Fig. 15 of Ref. [19].¹ Like other models, also this model fails to fit kaonic atoms data on its own. Adding a phenomenological density dependent amplitude produces fits with χ^2 of 150 for the 65 data points, which is significantly inferior to fits obtained for the chiral EFT models considered in Ref. [18].

It was shown in Ref. [18] that one could distinguish between different $\bar{K}N$ models by testing their ability to reproduce experimentally deduced values of single-nucleon absorption fractions at threshold across the periodic table. Fig. 1 shows such fractions as calculated for four models of the $\bar{K}N$ interaction, including that of Eq. (1). Results of calculated absorptions from

¹We thank Tetsuo Hyodo for providing us with tables of these amplitudes.

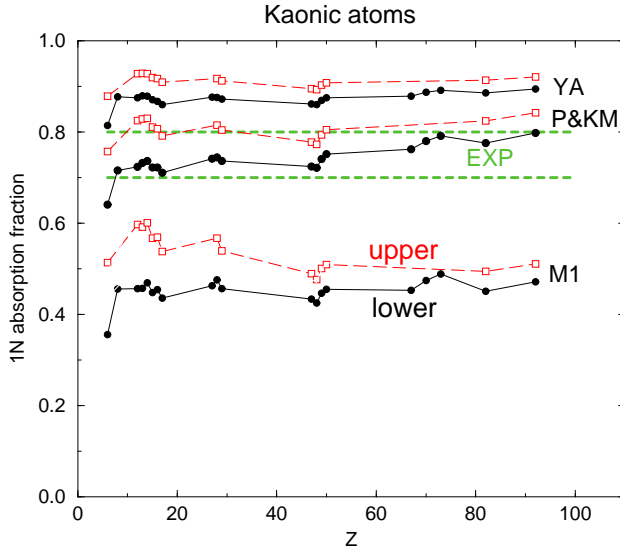


Figure 1: K^- single-nucleon absorption fractions calculated using K^-N amplitudes from the chiral EFT models M1, P and KM, see Ref. [18], and as generated from Eq. (1) (here marked YA). The range of experimentally deduced fractions, 0.70–0.80, is marked by horizontal dashed lines; see Ref. [18] for a comment on carbon (lowest Z points).

the so-called lower state and whenever provided by measured yields also from the upper state are shown for each kaonic atom. Experiments [20, 21, 22] do not distinguish directly between the two types of absorption.

As shown in the figure the $\bar{K}N$ interaction model of Eq. (1) (marked by YA) leads to far too large single-nucleon fractions whereas, for example, the Murcia (M1) model leads to too small ratios. The Kyoto-Munich (KM) model and the Prague (P) model, which yield predictions indistinguishable from each other, provide a very good agreement with experiment. The bottom line for the present discussion is that the $\bar{K}N$ interaction model of Eq. (1) does not reproduce the experimental absorption fractions.

4. RMF calculations of purely- Λ^* nuclei

Bound systems of Λ^* hyperons are treated here in a similar way as applied to nuclei [5] and also to hypernuclei, e.g. in Ref. [23], within the RMF framework. In our calculations of Λ^* nuclei, we employed the linear RMF model HS [24], taking into account the coupling of Λ^* baryons to isoscalar-scalar

σ and isoscalar-vector ω meson fields. Other fields considered in ordinary nuclei, such as isovector-vector $\vec{\rho}$ or Coulomb fields were disregarded since the Λ^* is a neutral $I = 0$ baryon. The resulting RMF model Lagrangian density for Λ^* nuclei is of the form ($\hbar = c = 1$ from now on):

$$\mathcal{L} = \bar{\Lambda}^* [i\gamma^\mu D_\mu - (M_{\Lambda^*} - g_{\sigma\Lambda^*}\sigma)] \Lambda^* + (\sigma, \omega_\mu \text{ free-field terms}), \quad (2)$$

where the covariant derivative $D_\mu = \partial_\mu + i g_{\omega\Lambda^*} \omega_\mu$ couples the vector meson field ω to the Λ^* baryon fields. Here we disregard the $\omega\Lambda^*$ tensor coupling term $f_{\omega\Lambda^*}\sigma_{\mu\nu}\omega_\nu$ which, while affecting spin-orbit splittings of single-particle levels, has little effect on the total binding energies of closed-shell nuclear systems (or Λ^* nuclei).

To start with, we used the HS linear model for atomic nuclei [24] with scalar and vector meson masses m_i ($i = \sigma, \omega$) and coupling constants g_{iN} given by

$$m_\sigma = 520 \text{ MeV}, \quad m_\omega = 783 \text{ MeV}, \quad g_{\sigma N} = 10.47, \quad g_{\omega N} = 13.80. \quad (3)$$

Modifying these coupling constants in ways described below, we explored Λ^* nuclei with closed shells by solving self-consistently the coupled system of the Klein-Gordon equations for meson fields and the Dirac equation for Λ^* .

In Fig. 2 we show binding energy values per baryon, B/A , calculated as a function of A for atomic nuclei (lowest two lines) and for purely Λ^* nuclei using mostly the linear HS model. It is clear that B/A saturates in all shown cases for $A \gtrsim 120$, to a value of order 10 MeV for nucleons when using parameters specified in Eq. (3), and to a somewhat higher value in the case of Λ^* nuclei (marked by Λ^*) upon using the same parameters. The increased B/A values in this case with respect to atomic nuclei is due to the higher Λ^* mass which reduces its kinetic energy. This is not yet the Λ^* matter calculation we should pursue since when extrapolated to $A = 2$ it gives a $B_{\Lambda^*\Lambda^*}$ value of only a few MeV, whereas the calculation pursued here assumes a considerably stronger $\Lambda^*\Lambda^*$ binding corresponding to $B(\bar{K}\bar{K}NN)_{I=0} - 2B(\bar{K}N)_{I=0} \approx 40$ MeV from column (E-indep.)_a in Table 1.² To renormalize the Λ^* RMF calculation to such a high value of $B_{\Lambda^*\Lambda^*}$ we need to increase $g_{\sigma N}$ or decrease $g_{\omega N}$ from the values listed in Eq. (3).

²We note for comparison that the scalar and vector Λ^* couplings estimated in the microscopic calculations of Ref. [28] within a chiral EFT model do not produce a bound $\Lambda^*\Lambda^*$ state.

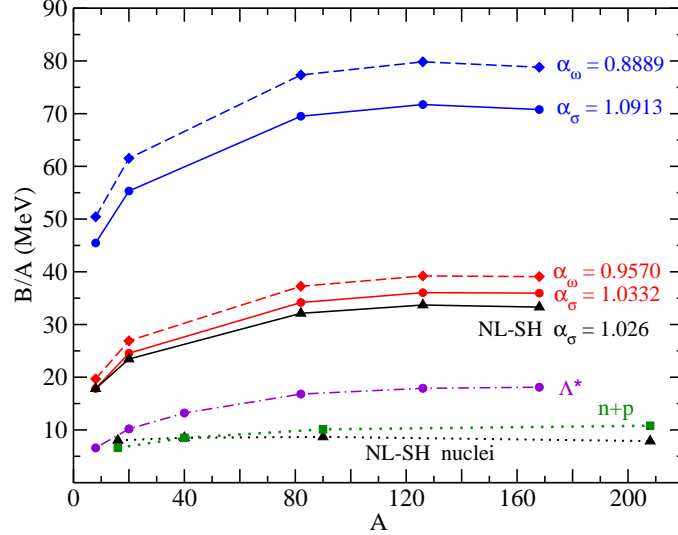


Figure 2: Binding energy of Λ^* nuclei per Λ^* , B/A as a function of mass number A , calculated within the HS and NL-SH RMF models for various strengths of scalar and vector fields (see text for details). The binding energy per nucleon in atomic nuclei is shown for comparison ($n + p$: HS without Coulomb and ρ meson field, NL-SH nuclei: including these terms).

This is how the other B/A lines marked by scaling factors α_σ or α_ω in Fig. 2 are obtained. The appropriate values of α_σ and α_ω are determined as follows.

The RMF underlying attractive scalar (σ) exchange and repulsive vector (ω) exchange baryon-baryon (BB) spin-singlet $S = 0$ potentials are given to lowest order in $(m/M)^2$ recoil corrections, disregarding tensor couplings, by:

$$V_{BB}(r) = g_{\omega B}^2 \left(1 - \frac{3}{8} \frac{m_\omega^2}{M_B^2}\right) Y_\omega(r) - g_{\sigma B}^2 \left(1 - \frac{1}{8} \frac{m_\sigma^2}{M_B^2}\right) Y_\sigma(r) \quad (4)$$

according to Dover-Gal [26], or

$$V_{BB}(r) = g_{\omega B}^2 Y_\omega(r) - g_{\sigma B}^2 \left(1 - \frac{1}{4} \frac{m_\sigma^2}{M_B^2}\right) Y_\sigma(r) \quad (5)$$

according to Machleidt [27]. Here $Y_i(r) = \exp(-m_i r)/(4\pi r)$ is the Yukawa form for meson exchange. The difference in the $(m/M)^2$ recoil terms in these two forms arises from a total neglect of nonlocal contributions in Dover-Gal, while partially retaining them by Machleidt. Using these BB= $\Lambda^*\Lambda^*$

potentials, with $M_{B=\Lambda^*} = 1405$ MeV, $\Lambda^*\Lambda^*$ binding energies were calculated by solving a two-body Schrödinger equation, scaling either $g_{\sigma N}$ or $g_{\omega M}$ according to $g_{\sigma N} \rightarrow g_{\sigma\Lambda^*} = \alpha_\sigma g_{\sigma N}$ and $g_{\omega N} \rightarrow g_{\omega\Lambda^*} = \alpha_\omega g_{\omega N}$ so as to get $B_{\Lambda^*\Lambda^*} = 40$ MeV while retaining the other coupling constant fixed. The resulting scaling parameters are listed in Table 2.

Table 2: Values of the scaling parameters α_σ and α_ω for σ and ω fields, respectively, each yielding $B_{\Lambda^*\Lambda^*} = 40$ MeV.

$V_{\Lambda^*\Lambda^*}$	α_σ	α_ω
Dover-Gal (4)	1.0332	0.9750
Machleidt (5)	1.0913	0.8889

We then performed RMF calculations of Λ^* nuclei using the renormalized coupling constants as marked to the right of each line in Fig. 2. Saturation is robust in all versions for $A \gtrsim 120$, but the saturation value depends on which potential version is used, Dover-Gal (4) or Machleidt (5). Scaling the ω meson coupling results in larger values of Λ^* binding energies than by scaling the σ meson coupling. Calculations were also performed using the nonlinear RMF model NL-SH [25] for comparison. The corresponding scaling parameter $\alpha_\sigma = 1.026$ was fitted to yield the binding energy of the $8\Lambda^*$ system calculated within the HS model for $\alpha_\sigma = 1.0332$. The resulting NL-SH calculation yields similar binding energies per Λ^* to those produced in the linear HS model. Fig. 2 clearly demonstrates that B/A does not exceed 100 MeV in any of the versions studied here. The calculated values are without exception considerably lower than the ≈ 290 MeV required to reduce the $\Lambda^*(1405)$ mass in the medium below that of the lightest hyperon $\Lambda(1116)$. This conclusion remains valid when Λ^* absorption is introduced in the present RMF calculations, say by considering the two-body conversion processes $\Lambda^*\Lambda^* \rightarrow YY$ ($Y = \Lambda, \Sigma$). Absorption normally translates into effective repulsion in bound state problems, thereby reducing the total binding energy and hence also the associated B/A values in Λ^* nuclei.

Having shown that B/A values saturate in Λ^* nuclei to values less than 100 MeV, we illustrate in Fig. 3 that the central density $\rho(r \approx 0)$ also saturates as a function of the mass number A . This is demonstrated in the left panel for the NL-SH model and $\alpha_\sigma = 1.026$. The central densities $\rho(0)$ shown in the figure vary in the range of $0.3\text{--}0.45$ fm $^{-3}$, which is about twice nuclear matter density. Expressing the r.m.s. radius of the Λ^* nuclear density dis-

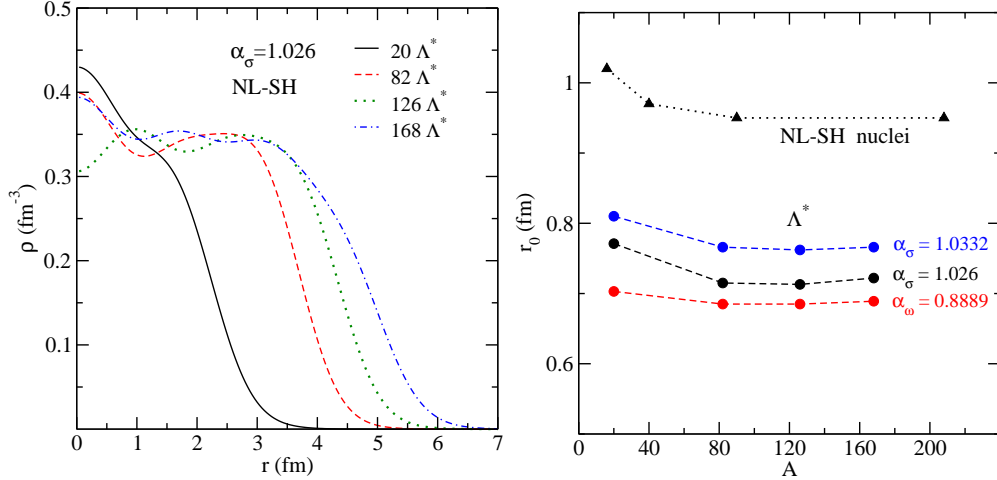


Figure 3: Left: Λ^* density distribution in systems composed of 20, 82, 126 and 168 Λ^* baryons, calculated within the NL-SH RMF model for $\alpha_\sigma = 1.026$. Right: values of the r.m.s. radius parameter r_0 in Λ^* nuclei (see text) for three of the RMF models and interaction strengths giving rise to B/A lines in Fig. 2. Values of r_0 in atomic nuclei (marked ‘NL-SH nuclei’) calculated within the NL-SH model are shown for comparison.

tribution ρ as $r_{\text{rms}} = r_0 A^{\frac{1}{3}}$, the variation of the radius parameter r_0 with A is shown in the right panel of the figure for selected $\Lambda^*\Lambda^*$ potential versions. Again, the radii r_0 saturate with values about 0.7–0.8 fm, indicating that Λ^* nuclei are more compressed than atomic nuclei in which r_0 is typically 0.9–1.0 fm, as shown by the upper line. The approximate constancy of r_0 with A is consistent with approximately uniform Λ^* matter density.

5. Conclusion

It was shown within a straightforward RMF calculation that the $\Lambda^*(1405)$ stable-matter scenario promoted by AY [3] is unlikely to be substantiated in standard many-body schemes. The decisive role of Lorentz covariance to produce saturation in the RMF calculations of binding energies and sizes reported in Sect. 4 is worth noting. Lorentz covariance introduces two types of baryon density, a scalar $\rho_S = \bar{B}B$ associated with the attractive σ meson field and a vector $\rho_V = \bar{B}\gamma_0 B$ associated with the repulsive ω meson field. Whereas ρ_V coincides with the conserved baryon density $B^\dagger B$ (denoted simply ρ on the l.h.s. of Fig. 3), ρ_S shrinks with respect to ρ_V in dense matter

by a multiplicative factor $M^*/E^* < 1$, where $M^* = M - g_{\sigma B}\langle\sigma\rangle < M$ is the baryon density-dependent effective mass, thereby damping the attraction from the scalar σ meson field [5]. Saturation in the RMF model is thus entirely a relativistic phenomenon. Calculations within the non-relativistic approach with static potentials such as (4) or (5) would lead to collapse of systems composed of sufficiently large number of Λ^* baryons, as it also holds for nucleons [29].

Doubts were also raised in the present work on the validity of using a very strong and energy-independent $\bar{K}N$ $I = 0$ dominated potential fitted directly to the position and width of the $\Lambda^*(1405)$ resonance. Similar potentials have been used by AY over the years to promote the case for strongly bound \bar{K} nuclear clusters, see Table 1 here, and thereby also to suggest strongly attractive $\Lambda^*\Lambda^*$ interactions that would according to them lead to absolutely stable Λ^* matter. It was shown in Sect. 3 here that such strong and energy-independent $\bar{K}N$ potentials do not pass the test of kaonic atoms, hence casting doubts on their applicability in describing higher density kaonic features. Having said it, we concede that a proper description of high density hadronic matter, considerably beyond the $\rho \approx 2\rho_0$ density regime reached in our own calculations, may require the introduction of additional, new interaction mechanisms such as proposed recently in Ref. [30].

Finally, we recall related RMF calculations of multi- \bar{K} nuclei [31] in which, for a given core nucleus, the resulting \bar{K} separation energy $B_{\bar{K}}$, as well as the associated nuclear and \bar{K} -meson densities, were found to saturate with the number of \bar{K} mesons ($\gtrsim 10$). Saturation appeared in that study robust against a wide range of variations, including the RMF nuclear model used and the type of boson fields mediating the strong interactions. In particular strange systems made of protons and K^- mesons, as similar as possible to aggregates of $\Lambda^*(1405)$ baryons, were found in that work to be less bound than other strange-matter configurations. Our findings are in good qualitative agreement with the conclusion reached there that the SU(3) octet hyperons (Λ , Σ , Ξ) provide, together with nucleons, for the lowest energy strange hadronic matter configurations [1].

Acknowledgements

J.H. and M.S. acknowledge financial support from the CTU-SGS Grant No. SGS16/243/OHK4/3T/14. The work of N.B. is supported by the Pazy Foundation and by the Israel Science Foundation grant No. 1308/16.

References

- [1] J. Schaffner, C.B. Dover, A. Gal, C. Greiner, H. Stöcker, Phys. Rev. Lett. 71 (1993) 1328; J. Schaffner, C.B. Dover, A. Gal, C. Greiner, D.J. Millener, H. Stöcker, Ann. Phys. 235 (1994) 35; J. Schaffner-Bielich, A. Gal, Phys. Rev. C 62 (2000) 034311.
- [2] D. Chatterjee, I. Vidaña, Eur. Phys. J. A 52 (2016) 29.
- [3] Y. Akaishi, T. Yamazaki, Phys. Lett. B 774 (2017) 522.
- [4] T. Yamazaki, Y. Akaishi, A. Doté, Phys. Lett. B 587 (2004) 167.
- [5] B.D. Serot, J.D. Walecka, Adv. Nucl. Phys. 16 (1986) 1, preceded by a more compact and accessible form in Phys. Lett. B 87 (1979) 172.
- [6] Y. Akaishi, T. Yamazaki, Phys. Rev. C 65 (2002) 044005.
- [7] T. Yamazaki, Y. Akaishi, Phys. Rev. C 76 (2007) 045201.
- [8] T. Hyodo, D. Jido, Prog. Part. Nucl. Phys. 67 (2012) 55.
- [9] N. Barnea, A. Gal, E.Z. Liverts, Phys. Lett. B 712 (2012) 132.
- [10] S. Maeda, Y. Akaishi, T. Yamazaki, Proc. Jpn. Acad. Ser. B 89 (2013) 418.
- [11] T. Yamazaki, et al., Phys. Rev. Lett. 104 (2010) 132502.
- [12] G. Agakishiev, et al., Phys. Lett. B 742 (2015) 242.
- [13] S. Ajimura, et al., submitted to PRL, arXiv:1805.12275 (nucl-ex).
- [14] U.-G. Meißner, T. Hyodo, *Pole Structure of the $\Lambda(1405)$ Region*, a PDG18 Review in M. Tanabashi, et al., Phys. Rev. D 98 (2018) 030001.
- [15] E. Friedman, A. Gal, Phys. Rep. 452 (2007) 89.
- [16] M. Bazzi, et al. (SIDDHARTA Collaboration), Phys. Lett. B 704 (2011) 113.
- [17] M. Bazzi, et al. (SIDDHARTA Collaboration), Nucl. Phys. A 881 (2012) 88.

- [18] E. Friedman, A. Gal, Nucl. Phys. A 959 (2017) 66.
- [19] T. Hyodo, W. Weise, Phys. Rev. C 77 (2008) 035204.
- [20] H. Davis, et al., Nuovo Cimento 53A (1968) 313.
- [21] J.W. Moulder, et al., Nucl. Phys. B 35 (1971) 332.
- [22] C. Vander Velde-Wilquet, et al., Nuovo Cimento 39A (1977) 538.
- [23] J. Mareš, B.K. Jennings, Phys. Rev. C 49 (1994) 2472.
- [24] C.J. Horowitz, B.D. Serot, Nucl. Phys. A 368 (1981) 503.
- [25] M.M. Sharma, M.A. Nagarajan, P. Ring, Phys. Lett. B 312 (1993) 377.
- [26] C.B. Dover, A. Gal, Prog. Part. Nucl. Phys. 12 (1984) 171.
- [27] R. Machleidt, Adv. Nucl. Phys. 19 (1989) 189.
- [28] T. Uchino, T. Hyodo, M. Oka, Nucl. Phys. A 868-869 (2011) 53.
- [29] M. Schäfer, et al., work in preparation.
- [30] W. Paeng, M. Rho, Phys. Rev. C 91 (2015) 015801.
- [31] D. Gazda, E. Friedman, A. Gal, J. Mareš, Phys. Rev. C 77 (2008) 045206.